ELSEVIER

International Journal of Solids and Structures 41 (2004) 4809–4825

INTERNATIONAL JOURNAL OF SOLIDS and STRUCTURES

www.elsevier.com/locate/ijsolstr

Nonlinear bending behavior of Reissner–Mindlin plates with free edges resting on tensionless elastic foundations

Hui-Shen Shen *, L. Yu

School of Civil Engineering and Mechanics, Shanghai Jiao Tong University, 1954 Hua Shan Road, Shanghai 200030, People's Republic of China

Received 12 April 2003; received in revised form 1 February 2004
Available online 9 April 2004

Abstract

A nonlinear bending analysis is presented for a Reissner–Mindlin plate with four free edges subjected to thermomechanical loads and resting on a tensionless elastic foundation of the Pasternak-type. The mechanical loads consist of transverse partially distributed loads and in-plane edge loads while the temperature field is assumed to exhibit a linear variation through the thickness of the plate. The material properties are assumed to be independent of temperature. The two cases of initially compressed plates and of initially heated plates are considered. The formulations are based on Reissner–Mindlin first order shear deformation plate theory and include the plate-foundation interaction and thermal effects. A set of admissible functions, which satisfy both geometrical and natural boundary conditions, are developed for the nonlinear bending analysis of moderately thick plates with four free edges. A two step perturbation technique is employed in conjunction with this set of admissible functions to determine the load-deflection and load-bending moment curves. An iterative scheme is developed to obtain numerical results without using any prior assumption for the shape of the contact region. The numerical illustrations concern moderately thick plates with four free edges resting on tensionless elastic foundations of the Pasternak-type, from which results for conventional elastic foundations are obtained as comparators. The results show that the nonlinear bending responses for the conventional and tensionless elastic foundation are quite different.

Keywords: Nonlinear bending; Reissner–Mindlin plate with free edges; Tensionless elastic foundation; Thermomechanical loads; Analytical–numerical method

1. Introduction

The nonlinear bending response of initially heated or initially compressed Reissner–Mindlin plates with four free edges subjected to transverse partially distributed loads and resting on a two-parameter elastic foundation was the subject of recent investigations (Shen, 1998b, 1999). In these studies the foundation is

* Corresponding author.
E-mail address: hsshen@mail.sjtu.edu.cn (H.-S. Shen).

0020-7683/$ - see front matter © 2004 Elsevier Ltd. All rights reserved.
doi:10.1016/j.ijsolstr.2004.02.013

assumed to be an attached foundation in which the plate cannot separate from the elastic medium, this means the foundation reacts in compression as well as in tension. However, the lift-off problem of a plate is much more plausible, when the edge of the plate is free.

Many linear bending studies for thin and moderately thick, circular and rectangular plates resting on a tensionless elastic foundation have been performed by Weitsman (1970), Villaggio (1983), Celep (1988a,b), Li and Dempsey (1988), Mishra and Chakrabarti (1996), Akbarov and Kocatürk (1997), Xiao (2001) and Silva et al. (2001). The solution method required to determine the response of such plates on tensionless foundations is complicated because the contact region is not known at the outset. All the aforementioned studies focused on the cases of linear bending problem and they concluded that the contact region remains constant and is independent of the load level. In contrast, Khathlan (1994) studied the large deflections of circular plates resting on a tensionless elastic foundation of the Winkler-type and concluded that as the transverse load increases the contact area tends to expand until full contact is reached. Hong et al. (1999) studied the large deflections of axisymmetric shells and circular plates subjected to a central concentrated load and resting on a tensionless elastic foundation. However, in these studies the formulations are based on the Kirchhoff–Love hypothesis and therefore the transverse shear deformations are not accounted for.

The present study extends the previous works (Shen, 1998b, 1999) to the case of moderately thick rectangular plates with four free edges resting on a tensionless elastic foundation of the Pasternak-type. The nonlinear bending behaviors of initially compressed or initially heated plates are re-examined. The mechanical loads consist of transverse partially distributed loads and in-plane edge loads while the temperature field is assumed to exhibit a linear variation through the thickness of the plate. The material properties are assumed to be independent of temperature. The formulations are based on Reissner–Mindlin first order shear deformation plate theory and include the plate-foundation interaction and thermal effects. A set of admissible functions, which satisfy both geometrical and natural boundary conditions, are developed for the nonlinear bending analysis of moderately thick plates with four free edges. A two step perturbation technique is employed in conjunction with this set of admissible functions to determine the load-deflection and load-bending moment curves. An iterative scheme is developed to obtain numerical results without using any prior assumption for the shape of the contact region.

2. Analytical formulations

Consider a rectangular thick plate with four free edges of length a, width b and thickness t, which rests on a tensionless elastic foundation. Let X, Y and Z be a set of coordinates with X and Y axes located in the middle plane of the plate and the Z-axis pointing downwards. The origin of the coordinate system is located at the center of the plate in the middle plane. The plate is exposed to a stationary temperature field $T(X, Y, Z)$ and/or transverse partially distributed load q in the shaded region, as shown in Fig. 1, combined with in-plane edge loads P_x in the X-direction and P_y in the Y-direction. The components of displacement of the middle surface along the X, Y and Z axes are designated by $\overline{U}$, $\overline{V}$ and $\overline{W}$. $\overline{\Psi}_x$ and $\overline{\Psi}_y$ are the mid-plane rotations of the normals about the Y and X axes, respectively. The foundation is represented by a two-parameter foundation model, that is, the reaction of the foundation is assumed to be $p = \overline{K}_1\overline{W} - \overline{K}_2\nabla^2\overline{W}$, where p is the force per unit area, $\overline{K}_1$ is the Winkler foundation stiffness, $\overline{K}_2$ is a constant showing the effect of the shear interactions of the vertical elements, ∇^2 is the Laplace operator in X and Y. This reaction, however, is only compressive and occurs only where $\overline{W}$ is positive. Let $\overline{F}(X, Y)$ be the stress function for the stress resultants defined by $\overline{N}_x = \overline{F}_{,yy}$, $\overline{N}_y = \overline{F}_{,xx}$ and $\overline{N}_{xy} = -\overline{F}_{,xy}$, where a comma denotes partial differentiation with respect to the corresponding coordinates.

From Reissner–Mindlin plate theory considering the first order shear deformation effect, including the plate-foundation interaction and thermal effects, the nonlinear differential equations of such plates in the von Kármán sense are

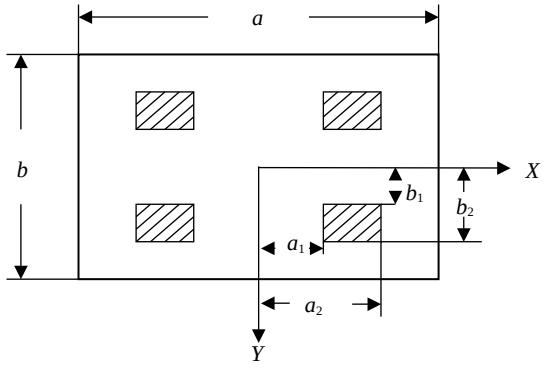

Fig. 1. A rectangular plate subjected to a transverse partially distributed load.

$$\widetilde{L}_{11}(\overline{\Psi}_x)+\widetilde{L}_{12}(\overline{\Psi}_y)+H(\overline{W})[\overline{K}_1\overline{W}-\overline{K}_2\nabla^2\overline{W}]+\nabla^2\overline{M}^{\mathrm{T}}=\widetilde{L}(\overline{W},\overline{F})+q \tag{1}$$

$$\widetilde{L}_{21}(\overline{\Psi}_x)+\widetilde{L}_{22}(\overline{\Psi}_y)+\widetilde{L}_{23}(\overline{W})+(\overline{M}^{\mathrm{T}})_{,x}=0 \tag{2}$$

$$\widetilde{L}_{31}(\overline{\Psi}_x)+\widetilde{L}_{32}(\overline{\Psi}_y)+\widetilde{L}_{33}(\overline{W})+(\overline{M}^{\mathrm{T}})_{,y}=0 \tag{3}$$

$$\nabla^4\overline{F}+(1-v)\nabla^2\overline{N}^{\mathrm{T}}=-\frac{1}{2}Et\widetilde{L}(\overline{W},\overline{W}) \tag{4}$$

where $H(\overline{W})$ is the contact function and takes care of the tensionless character of the foundation

$$H(\overline{W})=\begin{cases}1 & \overline{W}>0\\ 0 & \overline{W}\leqslant 0\end{cases} \tag{5}$$

and the linear operators $\widetilde{L}_{ij}(\ )$ and the nonlinear operator $\widetilde{L}(\ )$ are defined by

$$\begin{aligned}
\widetilde{L}_{11}(\ ) &= -D\frac{\partial}{\partial X}\nabla^2\\
\widetilde{L}_{12}(\ ) &= -D\frac{\partial}{\partial Y}\nabla^2\\
\widetilde{L}_{21}(\ ) &= \kappa^2Gt-D\left(\frac{\partial^2}{\partial X^2}+\frac{1-v}{2}\frac{\partial^2}{\partial Y^2}\right)\\
\widetilde{L}_{23}(\ ) &= \kappa^2Gt\frac{\partial}{\partial X}\\
\widetilde{L}_{31}(\ ) &= \widetilde{L}_{22}(\ ) = -\frac{1+v}{2}D\frac{\partial^2}{\partial X\partial Y}\\
\widetilde{L}_{32}(\ ) &= \kappa^2Gt-D\left(\frac{1-v}{2}\frac{\partial^2}{\partial X^2}+\frac{\partial^2}{\partial Y^2}\right)\\
\widetilde{L}_{33}(\ ) &= \kappa^2Gt\frac{\partial}{\partial Y}\\
\widetilde{L}(\ ) &= \frac{\partial^2}{\partial X^2}\frac{\partial^2}{\partial Y^2}-2\frac{\partial^2}{\partial X\partial Y}\frac{\partial^2}{\partial X\partial Y}+\frac{\partial^2}{\partial Y^2}\frac{\partial^2}{\partial X^2}\\
\nabla^2(\ ) &= \frac{\partial^2}{\partial X^2}+\frac{\partial^2}{\partial Y^2},\quad \nabla^4(\ )=\frac{\partial^4}{\partial X^4}+2\frac{\partial^4}{\partial X^2\partial Y^2}+\frac{\partial^4}{\partial Y^4}
\end{aligned} \tag{6}$$

in which D is flexural rigidity and $D = Et^3/12(1-v^2)$. E is Young's modulus, G is the shear modulus and v is Poisson's ratio. Also κ^2 is the shear factor, which accounts for the nonuniformity of the shear strain distribution through the plate thickness. For Reissner plate theory $\kappa^2 = 5/6$, while for Mindlin plate theory $\kappa^2 = \pi^2/12$.

If all four edges of the plate are free, the boundary conditions are

$X = \pm a/2$:

$$\overline{M}_x = D\left(\frac{\partial \overline{\Psi}_x}{\partial X} + v\frac{\partial \overline{\Psi}_y}{\partial Y}\right) - \overline{M}^{\mathrm{T}} = 0 \tag{7a}$$

$$\overline{M}_{xy} = \frac{1-v}{2}D\left(\frac{\partial \overline{\Psi}_x}{\partial Y} + \frac{\partial \overline{\Psi}_y}{\partial X}\right) = 0 \tag{7b}$$

$$\overline{Q}_x = \kappa^2 Gt\left(\overline{\Psi}_x + \frac{\partial \overline{W}}{\partial X}\right) = 0 \tag{7c}$$

$$\int_{-b/2}^{+b/2} \overline{N}_x \,\mathrm{d}Y + \sigma_x bt = 0 \tag{7d}$$

$Y = \pm b/2$:

$$\overline{M}_y = D\left(v\frac{\partial \overline{\Psi}_x}{\partial X} + \frac{\partial \overline{\Psi}_y}{\partial Y}\right) - \overline{M}^{\mathrm{T}} = 0 \tag{7e}$$

$$\overline{M}_{xy} = \frac{1-v}{2}D\left(\frac{\partial \overline{\Psi}_x}{\partial Y} + \frac{\partial \overline{\Psi}_y}{\partial X}\right) = 0 \tag{7f}$$

$$\overline{Q}_y = \kappa^2 Gt\left(\overline{\Psi}_y + \frac{\partial \overline{W}}{\partial Y}\right) = 0 \tag{7g}$$

$$\int_{-a/2}^{+a/2} \overline{N}_y \,\mathrm{d}X + \sigma_y at = 0 \tag{7h}$$

where σ_x and σ_y are the average compressive stresses in the X- and Y-directions, $\overline{M}_x$ and $\overline{M}_y$ are the bending moments per unit width and per unit length of the plate, and $\overline{Q}_x$ and $\overline{Q}_y$ are the transverse shear forces, respectively.

For the initially heated plate, it is assumed that $\sigma_x = \sigma_y = 0$ and the temperature field is assumed to be a linear variation through the plate thickness, i.e.

$$T(X,Y,Z) = T_0\left[1 + C\frac{Z}{t}\right] \tag{8}$$

in which T_0 and C denote the temperature amplitude and gradient respectively.

The thermal forces and moments caused by the temperature field $T(X,Y,Z)$ are defined by

$$(\overline{N}^{\mathrm{T}}, \overline{M}^{\mathrm{T}}) = \frac{E\alpha}{1-v}\int_{-t/2}^{+t/2} (1, Z)T(X,Y,Z)\,\mathrm{d}Z \tag{9}$$

where α is the thermal expansion coefficient of a plate.

Because of Eqs. (8) and (9), it is noted that the temperature does not vary in X and Y, then the thermal forces $\overline{N}^{\mathrm{T}}$ and moments $\overline{M}^{\mathrm{T}}$ are constants, so that the boundary conditions of Eqs. (7a) and (7e) are nonhomogeneous, but in Eqs. (1)–(4) $\nabla^2\overline{M}^{\mathrm{T}} = \nabla^2\overline{N}^{\mathrm{T}} = (\overline{M}^{\mathrm{T}})_{,x} = (\overline{M}^{\mathrm{T}})_{,y} = 0$.

For the initially compressed plate, it is assumed that $\overline{N}^{\mathrm{T}} = \overline{M}^{\mathrm{T}} = 0$, now the boundary conditions of Eqs. (7a) and (7e) become homogeneous.

3. Analytical method and solution procedure

Before proceeding, it is convenient first to define the following dimensionless quantities for such plates (in which the alternative forms k_1 and k_2 are not needed until the numerical examples are considered)

$$\begin{aligned}
&x = \pi X/a, \quad y = \pi Y/b, \quad \beta = a/b, \quad \gamma = \pi^2 D/a^2\kappa^2 G t, \quad (\nu_1, \nu_2) = (1-\nu, 1+\nu)/2\\
&(W, W^*) = (\overline{W}, \overline{W}^*)[12(1-\nu^2)]^{1/2}/t, \quad (\Psi_x, \Psi_y) = (\overline{\Psi}_x, \overline{\Psi}_y)a[12(1-\nu^2)]^{1/2}/\pi t\\
&F = \overline{F}/D, \quad (Q_x, Q_y) = (\overline{Q}_x, \overline{Q}_y)a[12(1-\nu^2)]^{1/2}/\pi\kappa^2 G t^2\\
&(M_x, M_y, M_{xy}, M^{\mathrm{T}}) = (\overline{M}_x, \overline{M}_y, \overline{M}_{xy}, \overline{M}^{\mathrm{T}})a^2[12(1-\nu^2)]^{1/2}/\pi^2 D t\\
&(K_1, k_1) = (a^4, b^4)\overline{K}_1/\pi^4 D, \quad (K_2, k_2) = (a^2, b^2)\overline{K}_2/\pi^2 D\\
&\lambda_q = qa^4[12(1-\nu^2)]^{1/2}/\pi^4 D t, \quad (\lambda_x, \lambda_y) = (\sigma_x b^2, \sigma_y a^2)t/4\pi^2 D
\end{aligned} \tag{10}$$

Eqs. (1)–(4) may then be written in dimensionless form as

$$L_{11}(\Psi_x) + L_{12}(\Psi_y) + H(W)[K_1 W - K_2\overline{\nabla}^2 W] = \beta^2 L(W, F) + \lambda_q \tag{11}$$

$$L_{21}(\Psi_x) + L_{22}(\Psi_y) + L_{23}(W) = 0 \tag{12}$$

$$L_{31}(\Psi_x) + L_{32}(\Psi_y) + L_{33}(W) = 0 \tag{13}$$

$$\overline{\nabla}^4 F = -\frac{1}{2}\beta^2 L(W, W) \tag{14}$$

where

$$\begin{aligned}
L_{11}(\,) &= -\frac{\partial}{\partial x}\overline{\nabla}^2\\
L_{12}(\,) &= -\beta\frac{\partial}{\partial y}\overline{\nabla}^2\\
L_{21}(\,) &= 1 - \gamma\left(\frac{\partial^2}{\partial x^2} + \nu_1\beta^2\frac{\partial^2}{\partial y^2}\right)\\
L_{23}(\,) &= \frac{\partial}{\partial x}\\
L_{31}(\,) &= L_{22}(\,) = -\nu_2\gamma\beta\frac{\partial^2}{\partial x\partial y}\\
L_{32}(\,) &= 1 - \gamma\left(\nu_1\frac{\partial^2}{\partial x^2} + \beta^2\frac{\partial^2}{\partial y^2}\right)\\
L_{33}(\,) &= \beta\frac{\partial}{\partial y}
\end{aligned}$$

$$L(\ ) = \frac{\partial^2}{\partial x^2}\frac{\partial^2}{\partial y^2} - 2\frac{\partial^2}{\partial x \partial y}\frac{\partial^2}{\partial x \partial y} + \frac{\partial^2}{\partial y^2}\frac{\partial^2}{\partial x^2}$$
$$\overline{\nabla}^2(\ ) = \frac{\partial^2}{\partial x^2} + \beta^2\frac{\partial^2}{\partial y^2}, \quad \overline{\nabla}^4(\ ) = \frac{\partial^4}{\partial x^4} + 2\beta^2\frac{\partial^4}{\partial x^2 \partial y^2} + \beta^4\frac{\partial^4}{\partial y^4} \tag{15}$$

The boundary conditions of Eq. (7) become

$x = \pm\pi/2$:

$$M_x = \left(\frac{\partial \Psi_x}{\partial x} + \nu\beta\frac{\partial \Psi_y}{\partial y}\right) - M^{\mathrm{T}} = 0 \quad \text{(for initially heated plate)} \tag{16a}$$

$$M_x = \left(\frac{\partial \Psi_x}{\partial x} + \nu\beta\frac{\partial \Psi_y}{\partial y}\right) = 0 \quad \text{(for initially compressed plate)} \tag{16a$'$}$$

$$M_{xy} = \nu_1\left(\beta\frac{\partial \Psi_x}{\partial y} + \frac{\partial \Psi_y}{\partial x}\right) = 0 \tag{16b}$$

$$Q_x = \left(\Psi_x + \frac{\partial W}{\partial x}\right) = 0 \tag{16c}$$

$$\frac{1}{\pi}\int_{-\pi/2}^{+\pi/2} \beta^2\frac{\partial^2 F}{\partial y^2}\,\mathrm{d}y = 0 \quad \text{(for initially heated plate)} \tag{16d}$$

$$\frac{1}{\pi}\int_{-\pi/2}^{+\pi/2} \beta^2\frac{\partial^2 F}{\partial y^2}\,\mathrm{d}y + 4\lambda_x\beta^2 = 0 \quad \text{(for initially compressed plate)} \tag{16d$'$}$$

$y = \pm\pi/2$:

$$M_y = \left(\nu\frac{\partial \Psi_x}{\partial x} + \beta\frac{\partial \Psi_y}{\partial y}\right) - M^{\mathrm{T}} = 0 \quad \text{(for initially heated plate)} \tag{16e}$$

$$M_y = \left(\nu\frac{\partial \Psi_x}{\partial x} + \beta\frac{\partial \Psi_y}{\partial y}\right) = 0 \quad \text{(for initially compressed plate)} \tag{16e$'$}$$

$$M_{xy} = \nu_1\left(\beta\frac{\partial \Psi_x}{\partial y} + \frac{\partial \Psi_y}{\partial x}\right) = 0 \tag{16f}$$

$$Q_y = \left(\Psi_y + \beta\frac{\partial W}{\partial y}\right) = 0 \tag{16g}$$

$$\frac{1}{\pi}\int_{-\pi/2}^{+\pi/2} \frac{\partial^2 F}{\partial x^2}\,\mathrm{d}x = 0 \quad \text{(for initially heated plate)} \tag{16h}$$

$$\frac{1}{\pi}\int_{-\pi/2}^{+\pi/2} \frac{\partial^2 F}{\partial x^2}\,\mathrm{d}x + 4\lambda_y = 0 \quad \text{(for initially compressed plate)} \tag{16h$'$}$$

Applying Eqs. (11)–(16), the nonlinear bending of an initially heated or initially compressed Reissner–Mindlin plate with four free edges subjected to combined loading and resting on a tensionless elastic foundation of the Pasternak-type is now determined by a two step perturbation technique, for which the small perturbation parameter has no physical meaning at the first step, and is then replaced by a dimensionless transverse pressure (or central deflection) at the second step. The essence of this procedure, in the present case, is to assume that

$$\begin{aligned} W(x,y,\varepsilon) &= \sum_{j=1} \varepsilon^j w_j(x,y), \quad \Psi_x(x,y,\varepsilon) = \sum_{j=1} \varepsilon^j \psi_{xj}(x,y) \\ \Psi_y(x,y,\varepsilon) &= \sum_{j=1} \varepsilon^j \psi_{yj}(x,y), \quad F(x,y,\varepsilon) = \sum_{j=0} \varepsilon^j f_j(x,y), \quad \lambda_q = \sum_{j=1} \varepsilon^j \lambda_j \end{aligned} \tag{17}$$

where ε is a small perturbation parameter.

In order to satisfy free boundary conditions, the first term of $w_j(x,y)$ is assumed to have the form

$$w_1(x,y) = A_{00}^{(1)} + A_{20}^{(1)} \cos 2mx + A_{02}^{(1)} \cos 2ny + A_{22}^{(1)} \cos 2mx \cos 2ny + a_1^{(1)} x^2 + a_2^{(1)} y^2 \tag{18}$$

in which, $A_{00}^{(1)}$, $A_{20}^{(1)}$, etc. are unknown coefficients.

All the necessary steps of the solution methodology are described below, but the detailed expressions are not shown, since they may be found in Shen (1998a, 2002).

First, the assumed solution form of Eq. (17) is substituted into Eqs. (11)–(14) to obtain a set of perturbation equations by collecting the terms of the same order of ε.

Then, Eq. (18) is used to solve these perturbation equations of each order step by step. At each step the amplitudes of the components of $w_j(x,y)$, $\psi_{xj}(x,y)$, $\psi_{yj}(x,y)$ and $f_j(x,y)$ can be determined, e.g. $A_{20}^{(1)}$, $A_{02}^{(1)}$, $B_{20}^{(2)}$, $B_{02}^{(2)}$, etc., except for $A_{00}^{(j)}$ $(j = 1, 3)$ and which along with λ_j can be determined by the Galerkin procedure. As a result, up to third-order asymptotic solutions are obtained as

$$\begin{aligned} W = {} & \varepsilon[A_{00}^{(1)} + A_{20}^{(1)} \cos 2mx + A_{02}^{(1)} \cos 2ny + A_{22}^{(1)} \cos 2mx \cos 2ny + a_1^{(1)} x^2 + a_2^{(1)} y^2] \\ & + \varepsilon^3 [A_{00}^{(3)} + A_{20}^{(3)} \cos 2mx + A_{02}^{(3)} \cos 2ny + A_{22}^{(3)} \cos 2mx \cos 2ny + A_{24}^{(3)} \cos 2mx \cos 4ny \\ & + A_{26}^{(3)} \cos 2mx \cos 6ny + A_{40}^{(3)} \cos 4mx + A_{42}^{(3)} \cos 4mx \cos 2ny + A_{44}^{(3)} \cos 4mx \cos 4ny \\ & + A_{46}^{(3)} \cos 4mx \cos 6ny + A_{04}^{(3)} \cos 4ny + A_{60}^{(3)} \cos 6mx + A_{62}^{(3)} \cos 6mx \cos 2ny \\ & + A_{64}^{(3)} \cos 6mx \cos 4ny + A_{06}^{(3)} \cos 6ny + a_1^{(3)} x^2 + a_2^{(3)} y^2] + \mathrm{O}(\varepsilon^4) \end{aligned} \tag{19}$$

$$\begin{aligned} \Psi_x = {} & \varepsilon[C_{20}^{(1)} \sin 2mx + C_{22}^{(1)} \sin 2mx \cos 2ny + c_1^{(1)} x] + \varepsilon^3 [C_{20}^{(3)} \sin 2mx + C_{22}^{(3)} \sin 2mx \cos 2ny \\ & + C_{24}^{(3)} \sin 2mx \cos 4ny + C_{26}^{(3)} \sin 2mx \cos 6ny + C_{40}^{(3)} \sin 4mx + C_{42}^{(3)} \sin 4mx \cos 2ny \\ & + C_{44}^{(3)} \sin 4mx \cos 4ny + C_{46}^{(3)} \sin 4mx \cos 6ny + C_{60}^{(3)} \sin 6mx + C_{62}^{(3)} \sin 6mx \cos 2ny \\ & + C_{64}^{(3)} \sin 6mx \cos 4ny + c_1^{(3)} x] + \mathrm{O}(\varepsilon^4) \end{aligned} \tag{20}$$

$$\begin{aligned} \Psi_y = {} & \varepsilon[D_{02}^{(1)} \sin 2ny + D_{22}^{(1)} \cos 2mx \sin 2ny + d_2^{(1)} y] + \varepsilon^3 [D_{02}^{(3)} \sin 2ny + D_{22}^{(3)} \cos 2mx \sin 2ny \\ & + D_{24}^{(3)} \cos 2mx \sin 4ny + D_{26}^{(3)} \cos 2mx \sin 6ny + D_{42}^{(3)} \cos 4mx \sin 2ny + D_{44}^{(3)} \cos 4mx \sin 4ny \\ & + D_{46}^{(3)} \cos 4mx \sin 6ny + D_{04}^{(3)} \sin 4ny + D_{62}^{(3)} \cos 6mx \sin 2ny + D_{64}^{(3)} \cos 6mx \sin 4ny \\ & + D_{06}^{(3)} \sin 6ny + d_1^{(3)} y] + \mathrm{O}(\varepsilon^4) \end{aligned} \tag{21}$$

$$F = -B_{00}^{(0)}\frac{y^2}{2} - b_{00}^{(0)}\frac{x^2}{2} + \varepsilon^2\left[- B_{00}^{(2)}\left(y^2 - \frac{\pi^2}{4}\right)^2 - b_{00}^{(2)}\left(x^2 - \frac{\pi^2}{4}\right)^2 + B_{20}^{(2)}\cos 2mx + B_{02}^{(2)}\cos 2ny \right.$$
$$+ B_{22}^{(2)}\cos 2mx\cos 2ny + B_{40}^{(2)}\cos 4mx + B_{04}^{(2)}\cos 4ny + B_{24}^{(2)}\cos 2mx\cos 4ny$$
$$\left. + B_{42}^{(2)}\cos 4mx\cos 2ny\right] + \mathrm{O}(\varepsilon^4) \tag{22}$$

and

$$\lambda_q = \varepsilon\lambda_1 + \varepsilon^3\lambda_3 + \mathrm{O}(\varepsilon^4) \tag{23}$$

It is because the isotropic plate with bending/stretching coupling missing, the terms in ε^0 and ε^2 in Eqs. (19)–(21), and the terms in ε^1 and ε^3 in Eq. (22) are all zero-valued. Note that in Eq. (22) $B_{00}^{(0)}$ and $b_{00}^{(0)}$ come from initial in-plane uniform compressive stresses, and for initially heated problem they are all zero-valued. All coefficients in Eqs. (19)–(23) are related and can be expressed in terms of $A_{22}^{(1)}$, for example, $A_{00}^{(1)} = \alpha_{100}A_{22}^{(1)}$, $A_{00}^{(3)} = \alpha_{300}A_{22}^{(1)}$ (with α_{100}, α_{300}, etc. defined in Appendix A), so that Eqs. (19) and (23) can be re-written as

$$W = W^{(1)}(x,y)(A_{22}^{(1)}\varepsilon) + W^{(3)}(x,y)(A_{22}^{(1)}\varepsilon)^3 + \cdots \tag{24}$$

and

$$\lambda_q = \lambda_q^{(1)}(A_{22}^{(1)}\varepsilon) + \lambda_q^{(3)}(A_{22}^{(1)}\varepsilon)^3 + \cdots \tag{25}$$

In Eqs. (24) and (25) $(A_{22}^{(2)}\varepsilon)$ is taken as the second perturbation parameter relating to the dimensionless transverse pressure. From Eqs. (24) and (25) the load-central deflection relationship can be written as

$$\frac{\overline{W}}{t} = A_W^{(1)}\left(\frac{qa^4}{Dt}\right) + A_W^{(3)}\left(\frac{qa^4}{Dt}\right)^3 + \cdots \tag{26}$$

Similarly, the load-bending moment relationships can be written as

$$\frac{\overline{M}_x a^2}{Dt} = A_{Mx}^{(0)} + A_{Mx}^{(1)}\left(\frac{qa^4}{Dt}\right) + A_{Mx}^{(3)}\left(\frac{qa^4}{Dt}\right)^3 + \cdots \tag{27}$$

$$\frac{\overline{M}_y a^2}{Dt} = A_{My}^{(0)} + A_{My}^{(1)}\left(\frac{qa^4}{Dt}\right) + A_{My}^{(3)}\left(\frac{qa^4}{Dt}\right)^3 + \cdots \tag{28}$$

Note that $A_{Mx}^{(0)}$ and $A_{My}^{(0)}$ are initial bending moments induced by temperature field and for initially compressed problem they are all zero-valued. In Eqs. (26)–(28), all coefficients are given in detail in Appendix A.

Eqs. (26)–(28) can be employed to obtain numerical results for the load-deflection and load-bending moment curves of an initially heated or initially compressed Reissner–Mindlin plate with four free edges subjected to combined loading and resting on tensionless elastic foundations. Since the foundation reacts in compression only, a possible lift-off region is expected. The solution procedure is complicated and therefore an iterative procedure is necessary to solve this strong nonlinear problem. In applying the contact condition, the plate area is discretized into a series of grids, and the contact status is assessed at each grid location. From Eq. (A.2) in Appendix A one can see some terms, e.g. C_{02}, C_{22}, g_{3i0}, g_{30j}, g_{3ij}, etc., involving K_1 and K_2 and the contact function $H[W(x_g,y_g)]$, where $W(x_g,y_g)$ is the deflection at the grid coordinate (x_g,y_g) and summation is carried out over all grid coordinates by using the Gauss–Legendre quadrature procedure. It is found that an acceptable accuracy can be obtained by taking into account 10×10 points, which is employed in the next section.

4. Numerical examples and discussions

Numerical results are presented in this section for initially compressed or initially heated moderately thick plates with four free edges subjected to a central patch load ($a_1 = b_1 = 0$) and resting on a tensionless elastic foundation of the Pasternak-type. The results for conventional elastic foundations are obtained as comparators in the manner described previously and detailed further in Shen (1998b, 1999). A computer program was developed for this purpose and many examples have been solved numerically, including the following.

The accuracy and effectiveness of the present method for linear and nonlinear bending analyses of moderately thick plates resting on a Winkler elastic foundation were examined by many comparison studies given in Shen (1998b, 1999), e.g. the deflections and bending moments along the X-axis for a moderately thick plate subjected to a central patch load were compared with the Fourier series solutions and finite-difference method results given by Henwood et al. (1982) and the superposition method solutions given by Shi et al. (1994), and the load-deflection curves for a moderately thick plates subjected to transverse partially distributed loads were compared with the classical plate theory solutions of Qu and Liang (1995). These comparisons show that the results from present method are in good agreement with existing results for the case of conventional elastic foundations. In addition, the central deflections and bending moments for moderately thick plates subjected to a central patch load and resting on both Winkler and tensionless elastic foundations (with $\overline{K}_1 = 50$ MN/m^3) are calculated and compared well in Table 1 with the Fourier series solutions obtained by Bu and Yan (1991), and boundary element method results of Xiao (2001). The computing data adopted here are $a = b = 4.0$ m, $t = 0.2$ m, $a_2 = b_2 = 0.25$ m, and $q_0 = 3.0$ MN/m^2. These results are based on the small deflection analysis and they confirm that the accuracy of the present analysis. As a second example, the central deflections and bending moments for moderately thick plates with three different kinds of material properties subjected to a central patch load and resting on Winkler elastic foundations (with $\overline{K}_1 = 20$, 50 and 80 MN/m^2) are calculated and compared in Table 2 with the Fourier Series solutions obtained by Yettram et al. (1984). The computing data adopted here are $a = b = 1.0$ m, $t = 0.05$ m, $a_2 = b_2 = 0.25$ m, and $q_0 = 1.0$ MN/m^2. It can be seen that the present results are lower than those of Yettram et al. (1984). The differences between these two solutions may be partly caused by different forms of deflection $\overline{W}$ chosen by different authors. In Table 2 results for tensionless elastic foundations are also given for direct comparison.

A parametric study was undertaken for a moderately thick square plate with $b/t = 20$. The transverse central patch load with $a_2/a = b_2/b = 0.25$ is applied on the top surface of the plate. Typical results are shown in Figs. 2–7. In all these figures $\overline{W}/t$ and $\overline{M}_x b^2/Et^4$ mean the dimensionless forms of, respectively, central deflection and bending moment of the plate, i.e. at the point $(X, Y) = (0, 0)$. For all of the examples, $E = 14.0$ GPa, $v = 0.15$, $\alpha = 1.0 \times 10^{-5}$/°C, and the transverse shear correction factor was taken to be $\kappa^2 = 5/6$.

Fig. 2 gives the load-deflection and load-bending moment curves for a moderately thick square plate subjected to a central patch load alone and resting on a tensionless elastic foundation of either

Table 1
Comparisons of central deflections and bending moments of partially loaded square plates ($a = b = 400$ cm, $t = 20$ cm, $a_2/a = b_2/b = 0.0625$, $q = 300$ N/cm^2, $E = 2.6 \times 10^6$ N/cm^2, $v = 0.15$, $\overline{K}_1 = 50$ N/cm^3)

	Winkler foundation		Tensionless foundation	
	$\overline{W}$ (cm)	$\overline{M}_x$ ($\times 10^5$ N cm)	$\overline{W}$ (cm)	$\overline{M}_x$ ($\times 10^5$ N cm)
Present	0.333981	0.106934	0.357982	0.118892
Bu and Yan (1991)	0.337788	0.116690	0.341402	0.118305
Xiao (2001)	0.341456	0.117297	0.346120	0.119732

Table 2
Comparisons of central deflections and bending moments of partially loaded square plates ($a = b = 1$ m, $t = 0.05$ m, $a_2/a = b_2 = b = 0.25$, $q = 1$ MN/m^2)

$\overline{K}_1$		Winkler foundation		Tensionless foundation	
		$\overline{W}$ (m)	$\overline{M}_x$ (MN m/m)	$\overline{W}$ (m)	$\overline{M}_x$ (MN m/m)
E = 3.0 GPa, v = 0.3					
20	Yettram et al. (1984)	0.0280	0.0120		
	Present	0.0265	0.0102	0.0270	0.0105
50	Yettram et al. (1984)	0.0145	0.00778		
	Present	0.0133	0.00602	0.0144	0.00688
80	Yettram et al. (1984)	0.0102	0.00590		
	Present	0.00895	0.00425	0.00991	0.00495
E = 6.85 GPa, v = 0.25					
20	Yettram et al. (1984)	0.0219	0.0150		
	Present	0.0213	0.0135	0.0213	0.0135
50	Yettram et al. (1984)	0.0117	0.0105		
	Present	0.0111	0.00934	0.0113	0.0973
80	Yettram et al. (1984)	0.0084	0.0089		
	Present	0.0078	0.00711	0.00823	0.00782
E = 14.0 GPa, v = 0.15					
20	Yettram et al. (1984)	0.0183	0.0163		
	Present	0.0179	0.0146	0.0179	0.0146
50	Yettram et al. (1984)	0.0100	0.0131		
	Present	0.00923	0.0114	0.00927	0.0115
80	Yettram et al. (1984)	0.00690	0.0111		
	Present	0.00658	0.00927	0.00671	0.00963

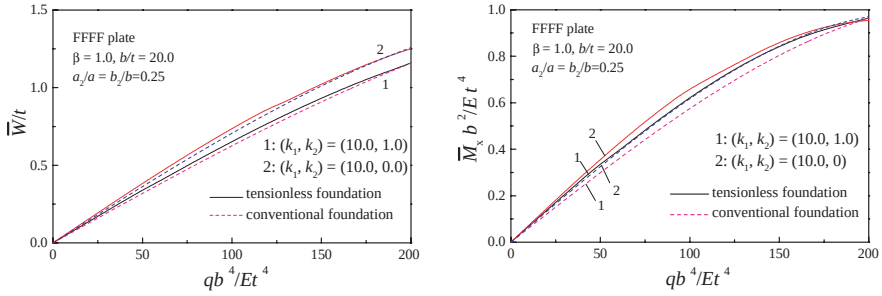

(a) load-deflection (b) load-bending moment

Fig. 2. Nonlinear bending behavior of a Reissner–Mindlin plate subjected to a central patch load resting on tensionless and conventional foundations.

Pasternak-type or Winkler-type. The stiffnesses are $(k_1, k_2) = (10.0, 1.0)$ for Pasternak-type elastic foundation and $(k_1, k_2) = (10.0, 0.0)$ for Winkler-type elastic foundation. It can be seen that the plate will have stronger nonlinear behavior than its counterparts when it is supported by a tensionless elastic foundation.

Fig. 3 gives the load-deflection and load-bending moment curves for a moderately thick square plate subjected to a central patch load combined with initial compressive load P_x resting on tensionless elastic foundations. The dimensionless uniaxial compression is defined by $P_x/P_{cr} = 0.25$, in which P_{cr} is the critical buckling load for the plate under uniaxial compression in the X-direction, and can be determined using the method described in Shen (2001) and Li (2000, 2001). Then Fig. 4 shows the effect of biaxial load ratio α_0

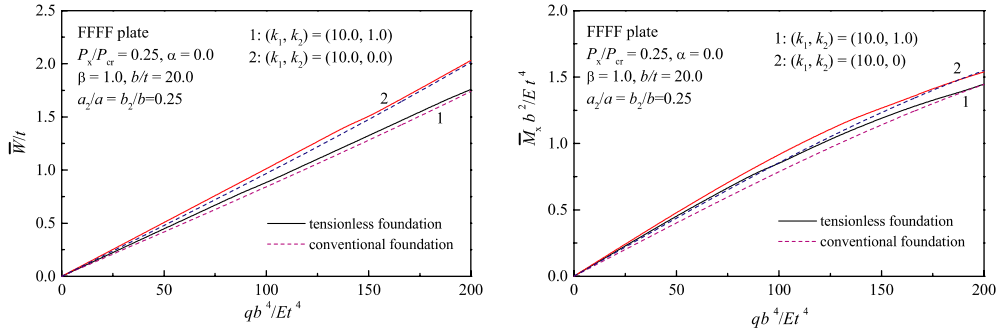

(a) load-deflection (b) load-bending moment

Fig. 3. Effect of initial uniaxial compression on the nonlinear bending behavior of a Reissner–Mindlin plate resting on conventional and tensionless foundations.

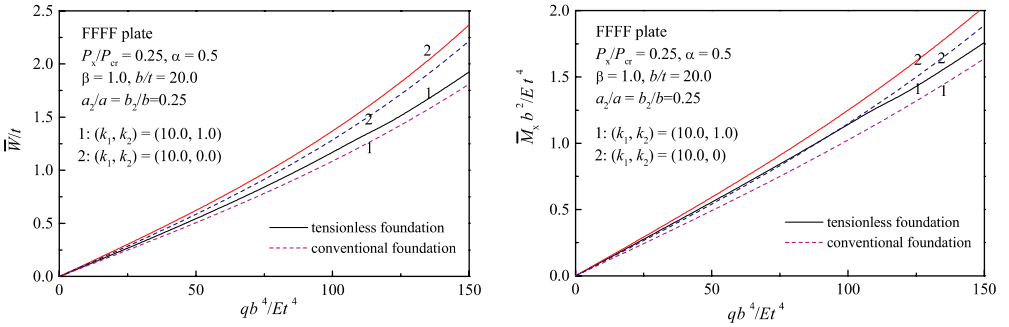

(a) load-deflection (b) load-bending moment

Fig. 4. Effect of initial biaxial compression on the nonlinear bending behavior of a Reissner–Mindlin plate resting on conventional and tensionless foundations.

$(= \sigma_y/\sigma_x = 0.5)$ on the nonlinear bending behavior of an initially compressed plate subjected to a central patch load resting on tensionless elastic foundations. It can be seen that for the initially compressed plate the load-deflection curve changes from convex to concave as the biaxial load ratio α_0 increases and the nonlinear effect becomes more pronounced as the applied load is increased.

Fig. 5 gives the load-deflection and load-bending moment curves for a moderately thick square plate subjected to a central patch load combined with uniform temperature rise $T_0 = 30$ °C and resting on tensionless elastic foundations. Then Fig. 6 shows the effect of thermal bending stress ($C = -2.0$) on the nonlinear bending behavior of an initially heated plate subjected to a central patch load resting on tensionless elastic foundations. As expected, these results show that in the case of low-valued uniform temperature rise the thermal stresses only have a small effect on the nonlinear bending behavior of the plate, even though the reaction of the foundation is in compression only.

Vertical deflections of the same plate subjected to a central patch load alone and under different load levels ($q^* = 50$, 100 and 200) are shown in Fig. 7. In Fig. 7 the dimensionless applied load is defined by $q^* = qb^4/Et^4$. The results show that at the plate central area the downward deflections of the plate resting on tensionless foundations are larger than those of the plate resting on conventional foundations when the applied load $q^* = 50$ and 100. Also the difference between these two curves becomes negligible at the plate

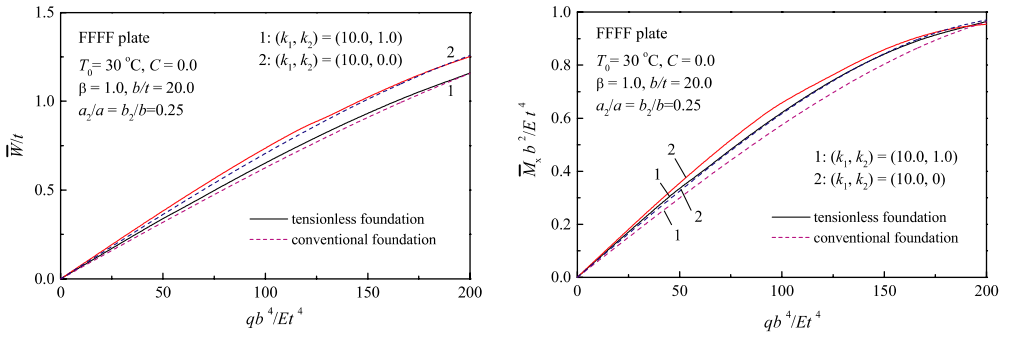

(a) load-deflection (b) load-bending moment

Fig. 5. Effect of initial uniform temperature rise on the nonlinear bending behavior of a Reissner–Mindlin plate resting on conventional and tensionless foundations.

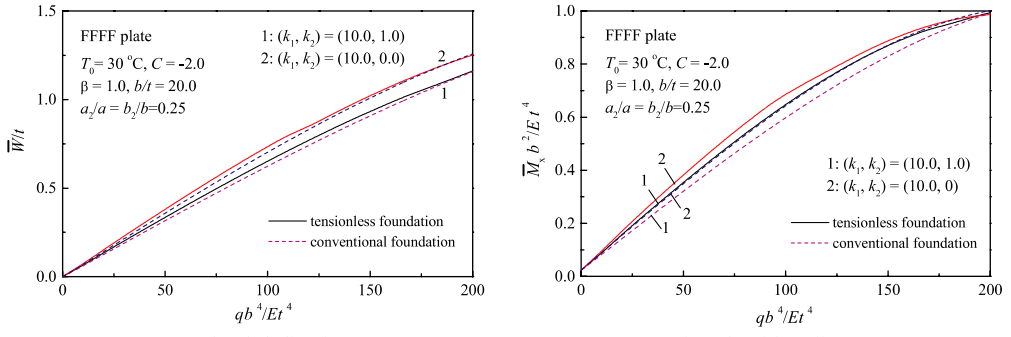

(a) load-deflection (b) load-bending moment

Fig. 6. Effect of thermal bending stress on the nonlinear bending behavior of a Reissner–Mindlin plate resting on conventional and tensionless foundations.

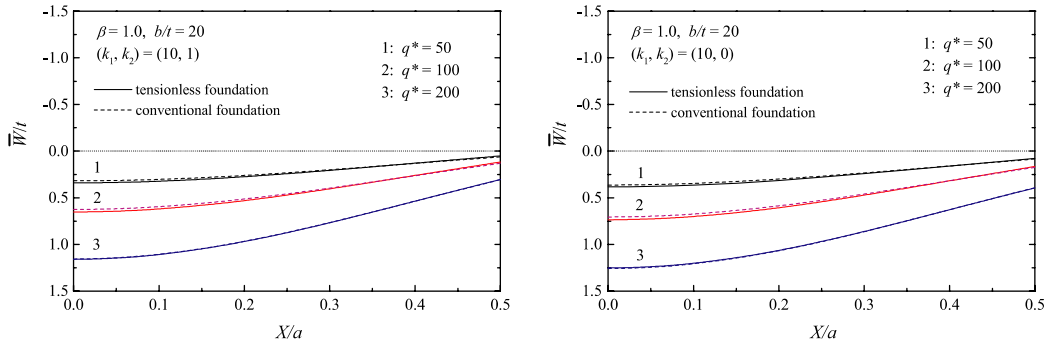

(a) Pasternak-type foundations (b) Winkler-type foundations

Fig. 7. Vertical deflections of a Reissner–Mindlin plate subjected to a central patch load resting on tensionless and conventional foundations.

edge region. In contrast, for the case of the applied load $q^* = 200$, these two curves are very close, confirming the contact region expands as the applied load increases.

5. Conclusions

Nonlinear bending analysis of an initially heated or initially compressed Reissner–Mindlin plate with four free edges subjected to transverse partially distributed loads and resting on a tensionless elastic foundation has been presented by using an analytical–numerical method. The advantage of the present method is that the solution is in an explicit form which is easy to program in computing full nonlinear load-deflection and load-bending moment curves without any prior assumption for the shape of the contact region. The new finding is that the nonlinear bending responses for the conventional and tensionless elastic foundation are quite different, and in the case of lift-off the stronger nonlinear response could be seen. The numerical results show that, due to the large deflection of the plate, the contact region expands as the applied load increases.

It is hoped that the results presented will contribute to a better understanding of the nonlinear bending behavior of Reissner–Mindlin plates with four free edges subjected to thermomechanical loads and resting on tensionless elastic foundations.

Acknowledgement

This work is supported in part by the National Natural Science Foundation of China under Grant 50375091. The authors are grateful for this financial support.

Appendix A

In Eqs. (26)–(28)

$$
\begin{aligned}
&A_W^{(1)} = C_1 W^{(1)}(x,y), \quad A_W^{(3)} = C_3 W^{(3)}(x,y) - C_2 W^{(1)}(x,y)\\
&A_{Mx}^{(1)} = \pi^2 C_1 M_x^{(1)}(x,y), \quad A_{Mx}^{(3)} = \pi^2 [C_3 M_x^{(3)}(x,y) - C_2 M_x^{(1)}(x,y)]\\
&A_{My}^{(1)} = \pi^2 C_1 M_y^{(1)}(x,y), \quad A_{My}^{(3)} = \pi^2 [C_3 M_y^{(3)}(x,y) - C_2 M_y^{(1)}(x,y)]\\
&W^{(1)}(x,y) = \alpha_{100} + \alpha_{120}\cos 2mx + \alpha_{102}\cos 2ny + \cos 2mx \cos 2ny + \alpha_{11}x^2 + \alpha_{12}y^2\\
&W^{(3)}(x,y) = \alpha_{300} + \alpha_{320}\cos 2mx + \alpha_{302}\cos 2ny + \alpha_{322}\cos 2mx \cos 2ny\\
&\qquad + \alpha_{324}\cos 2mx \cos 4ny + \alpha_{326}\cos 2mx \cos 6ny + \alpha_{340}\cos 4mx\\
&\qquad + \alpha_{342}\cos 4mx \cos 2ny + \alpha_{344}\cos 4mx \cos 4ny + \alpha_{346}\cos 4mx \cos 6ny\\
&\qquad + \alpha_{304}\cos 4ny + \alpha_{360}\cos 6mx + \alpha_{362}\cos 6mx \cos 2ny + \alpha_{364}\cos 6mx \cos 4ny\\
&\qquad + \alpha_{306}\cos 6ny + \alpha_{31}x^2 + \alpha_{32}y^2\\
&M_x^{(1)}(x,y) = \beta_{120}\cos 2mx + \beta_{102}\cos 2ny + \beta_{122}\cos 2mx \cos 2ny + 2\alpha_{11} + 2\nu n^2\beta^2\alpha_{12}\\
&M_x^{(3)}(x,y) = \beta_{320}\cos 2mx + \beta_{302}\cos 2ny + \beta_{322}\cos 2mx \cos 2ny\\
&\qquad + \beta_{324}\cos 2mx \cos 4ny + \beta_{326}\cos 2mx \cos 6ny + \beta_{340}\cos 4mx\\
&\qquad + \beta_{342}\cos 4mx \cos 2ny + \beta_{344}\cos 4mx \cos 4ny + \beta_{346}\cos 4mx \cos 6ny\\
&\qquad + \beta_{304}\cos 4ny + \beta_{360}\cos 6mx + \beta_{362}\cos 6mx \cos 2ny + \beta_{364}\cos 6mx \cos 4ny\\
&\qquad + \beta_{306}\cos 6ny + 2\alpha_{31} + 2\nu n^2\beta^2\alpha_{32}\\
&M_y^{(1)}(x,y) = \gamma_{120}\cos 2mx + \gamma_{102}\cos 2ny + \gamma_{122}\cos 2mx \cos 2ny + 2\nu\alpha_{11} + 2n^2\beta^2\alpha_{12}\\
&M_y^{(3)}(x,y) = \gamma_{320}\cos 2mx + \gamma_{302}\cos 2ny + \gamma_{322}\cos 2mx \cos 2ny\\
&\qquad + \gamma_{324}\cos 2mx \cos 4ny + \gamma_{326}\cos 2mx \cos 6ny + \gamma_{340}\cos 4mx\\
&\qquad + \gamma_{342}\cos 4mx \cos 2ny + \gamma_{344}\cos 4mx \cos 4ny + \gamma_{346}\cos 4mx \cos 6ny\\
&\qquad + \gamma_{304}\cos 4ny + \gamma_{360}\cos 6mx + \gamma_{362}\cos 6mx \cos 2ny + \gamma_{364}\cos 6mx \cos 4ny\\
&\qquad + \gamma_{306}\cos 6ny + 2\nu\alpha_{31} + 2n^2\beta^2\alpha_{32}
\end{aligned}
\tag{A.1}
$$

where (with all other symbols as defined in Shen (1998b, 1999))

$$
\begin{aligned}
C_{02} &= \frac{16m^4}{1+4\gamma m^2}\left(\alpha_{120}-\frac{1}{m^2}\alpha_{11}\cos m\pi\right)\alpha_{120}+\frac{16n^4\beta^4}{1+4\gamma n^2\beta^2}\left(\alpha_{102}-\frac{1}{n^2}\alpha_{12}\cos n\pi\right)\alpha_{102}\\
&\quad+8(m^2+n^2\beta^2)g_{22}+\sum_{g=0}^{N}C_g^{(N)}H[W(x_g,y_g)][K_1C_{021}+K_2C_{022}]\\
C_{22} &= g_{320}\alpha_{320}^2+g_{302}\alpha_{302}^2+\frac{1}{2}g_{322}\alpha_{322}^2+g_{340}\alpha_{340}^2+g_{304}\alpha_{304}^2+g_{360}\alpha_{360}^2+g_{306}\alpha_{306}^2\\
&\quad-\left(\frac{1}{m^2}g_{320}\alpha_{320}\cos m\pi+\frac{1}{4m^2}g_{340}\alpha_{340}+\frac{1}{9m^2}g_{360}\alpha_{360}\cos m\pi\right)\alpha_{31}\\
&\quad-\left(\frac{1}{n^2}g_{302}\alpha_{302}\cos n\pi+\frac{1}{4n^2}g_{304}\alpha_{304}+\frac{1}{9n^2}g_{306}\alpha_{306}\cos n\pi\right)\alpha_{32}\\
&\quad+C_{320}\alpha_{320}+C_{302}\alpha_{302}+\frac{1}{2}C_{322}\alpha_{322}+C_{340}\alpha_{340}+C_{304}\alpha_{304}+C_{360}\alpha_{360}+C_{306}\alpha_{306}\\
&\quad-\left(\frac{1}{m^2}C_{320}\cos m\pi+\frac{1}{4m^2}C_{340}+\frac{1}{9m^2}C_{360}\cos m\pi\right)\alpha_{31}\\
&\quad-\left(\frac{1}{n^2}C_{302}\cos n\pi+\frac{1}{4n^2}C_{304}+\frac{1}{9n^2}C_{306}\cos n\pi\right)\alpha_{32}\\
&\quad+\frac{4\beta^2}{1+\beta^2}\alpha_{11}\alpha_{12}\Bigg[-\left(\alpha_{120}\frac{m^2}{n^2}\cos n\pi+\alpha_{102}\frac{n^2\beta^2}{m^2}\cos m\pi\right)\alpha_{322}-\frac{1}{8}\left(\frac{m^2}{n^2}+\frac{n^2\beta^2}{m^2}\right)\alpha_{322}\\
&\qquad-\alpha_{320}\frac{m^2}{n^2}\cos n\pi-\alpha_{302}\frac{n^2\beta^2}{m^2}\cos m\pi+\left(\alpha_{31}\frac{1}{n^2}+\alpha_{32}\frac{\beta^2}{m^2}\right)\cos(m+n)\pi\\
&\qquad-\left(\alpha_{302}\frac{1}{n^2}\cos n\pi+\alpha_{304}\frac{1}{4n^2}+\alpha_{306}\frac{1}{9n^2}\cos n\pi\right)\alpha_{11}\\
&\qquad-\left(\alpha_{320}\frac{\beta^2}{m^2}\cos m\pi+\alpha_{340}\frac{1}{4m^2}+\alpha_{306}\frac{\beta^2}{9m^2}\cos m\pi\right)\alpha_{12}+\frac{\pi^4}{90}(\alpha_{11}\alpha_{32}+\alpha_{12}\alpha_{31}\beta^2)\Bigg]\\
&\quad+\sum_{g=0}^{N}C_g^{(N)}H[W(x_g,y_g)][K_1C_{221}+K_2C_{222}]+C_{224}
\end{aligned}
$$

$$\alpha_{120}=-\frac{1}{\nu m^2}(\nu m^2+n^2\beta^2)(1+4\gamma m^2)g_{22}\cos n\pi$$

$$\alpha_{102}=-\frac{1}{\nu n^2\beta^2}(m^2+\nu n^2\beta^2)(1+4\gamma n^2\beta^2)g_{22}\cos m\pi$$

$$\alpha_{11}=\frac{2}{\nu}n^2\beta^2 g_{22}\cos(m+n)\pi,\quad \alpha_{12}=\frac{2}{\nu\beta^2}m^2 g_{22}\cos(m+n)\pi$$

$$g_{3i0}=\frac{i^4m^4}{1+\gamma i^2m^2}+\sum_{g=0}^{N}C_g^{(N)}H[W(x_g,y_g)][K_1+K_2i^2m^2]-C_{310}\quad(i=2,4,6)$$

$$g_{30j}=\frac{j^4n^4\beta^4}{1+\gamma j^2n^2\beta^2}+\sum_{g=0}^{N}C_g^{(N)}H[W(x_g,y_g)][K_1+K_2j^2n^2\beta^2]-C_{301}\quad(j=2,4,6)$$

$$g_{3ij}=(i^2m^2+j^2n^2\beta^2)^2g_{ij}+\sum_{g=0}^{N}C_g^{(N)}H[W(x_g,y_g)][K_1+K_2(i^2m^2+j^2n^2\beta^2)]-C_{311}\quad(i,j=2,4,6)$$

$$g_{ij}=\frac{1}{1+\gamma(i^2m^2+j^2n^2\beta^2)}\quad(i,j=2,4,6)$$

$$\alpha_{324} = -\frac{1}{g_{324}}\left[6m^4\alpha_{120} + 4m^4\alpha_{102}\alpha_{11} + \frac{4m^2n^2\beta^2}{(m^2+n^2\beta^2)^2}(n^2\beta^2\alpha_{11} + m^2\beta^2\alpha_{12} + 2m^2n^2\beta^2\alpha_{120}\alpha_{102})\alpha_{102}\right.$$
$$\left. + \frac{4m^2n^2\beta^2}{(m^2+4n^2\beta^2)^2}(4n^2\beta^2\alpha_{11} + m^2\beta^2\alpha_{12})\alpha_{102} + \frac{18m^4n^4\beta^4}{(4m^2+n^2\beta^2)^2}\alpha_{120}\right]$$

$$\alpha_{326} = -\frac{1}{g_{326}}\left[m^4 + \frac{4m^4n^4\beta^4}{(m^2+4n^2\beta^2)^2}\alpha_{102}^2\right]$$

$$\alpha_{342} = -\frac{1}{g_{342}}\left[6n^4\beta^4\alpha_{102} + 4n^2\beta^4\alpha_{120}\alpha_{12} + \frac{4m^2n^2\beta^2}{(m^2+n^2\beta^2)^2}(n^2\beta^2\alpha_{11} + m^2\beta^2\alpha_{12} + 2m^2n^2\beta^2\alpha_{120}\alpha_{102})\alpha_{120}\right.$$
$$\left. + \frac{4m^2n^2\beta^2}{(4m^2+n^2\beta^2)^2}(n^2\beta^2\alpha_{11} + 4m^2\beta^2\alpha_{12})\alpha_{120} + \frac{18m^4n^4\beta^4}{(m^2+4n^2\beta^2)^2}\alpha_{102}\right]$$

$$\alpha_{344} = -\frac{16}{g_{344}}\left[\frac{m^4n^4\beta^4}{(m^2+4n^2\beta^2)^2} + \frac{m^4n^4\beta^4}{(4m^2+n^2\beta^2)^2}\right]\alpha_{120}\alpha_{102}$$

$$\alpha_{346} = -\frac{1}{g_{346}}\frac{2m^4n^4\beta^4}{(m^2+4n^2\beta^2)^2}\alpha_{102}$$

$$\alpha_{362} = -\frac{1}{g_{362}}\left[n^4\beta^4 + \frac{4m^4n^4\beta^4}{(4m^2+n^2\beta^2)^2}\alpha_{120}^2\right]$$

$$\alpha_{364} = -\frac{1}{g_{364}}\frac{2m^4n^4\beta^4}{(4m^2+n^2\beta^2)^2}\alpha_{120}$$

$$\alpha_{340} = -\frac{1+16\gamma m^2}{4\nu m^2}\left[(4\nu m^2 + n^2\beta^2)g_{42}\alpha_{342}\cos n\pi + 4(\nu m^2 + n^2\beta^2)g_{44}\alpha_{344}\right.$$
$$\left. + (4\nu m^2 + 9n^2\beta^2)g_{46}\alpha_{346}\cos n\pi\right]$$

$$\alpha_{304} = -\frac{1+16\gamma n^2\beta^2}{4\nu n^2\beta^2}\left[(m^2 + 4\nu n^2\beta^2)g_{24}\alpha_{324}\cos m\pi + 4(m^2 + \nu n^2\beta^2)g_{44}\alpha_{344}\right.$$
$$\left. + (9m^2 + 4\nu n^2\beta^2)g_{64}\alpha_{364}\cos m\pi\right],$$

$$\alpha_{360} = -\frac{1+36\gamma m^2}{9\nu m^2}\left[(9\nu m^2 + n^2\beta^2)g_{62}\alpha_{362}\cos n\pi + (9\nu m^2 + 4n^2\beta^2)g_{64}\alpha_{364}\right],$$

$$\alpha_{306} = -\frac{1+36\gamma n^2\beta^2}{9\nu n^2\beta^2}\left[(m^2 + 9\nu n^2\beta^2)g_{26}\alpha_{326}\cos m\pi + (4m^2 + 9\nu n^2\beta^2)g_{46}\alpha_{346}\right]$$

$$\alpha_{320} = -\frac{1+4\gamma m^2}{\nu m^2}\left[(\nu m^2 + n^2\beta^2)g_{22}\alpha_{322}\cos n\pi + (\nu m^2 + 4n^2\beta^2)g_{24}\alpha_{324}\right.$$
$$\left. + (\nu m^2 + 9n^2\beta^2)g_{26}\alpha_{326}\cos n\pi\right]$$

$$\alpha_{302} = -\frac{1+4\gamma n^2\beta^2}{\nu n^2\beta^2}\left[(m^2 + \nu n^2\beta^2)g_{22}\alpha_{322}\cos m\pi + (4m^2 + \nu n^2\beta^2)g_{42}\alpha_{342}\right.$$
$$\left. + (9m^2 + \nu n^2\beta^2)g_{62}\alpha_{362}\cos m\pi\right]$$

$$\begin{aligned}
\alpha_{31} &= -\frac{1}{2(1-v^2)}\left[\left(\frac{4m^2}{1+4\gamma m^2}\alpha_{320}\cos m\pi + \frac{16m^2}{1+16\gamma m^2}\alpha_{340} + \frac{36m^2}{1+36\gamma m^2}\alpha_{360}\cos m\pi\right)\right.\\
&\quad \left. - v\left(\frac{4n^2\beta^2}{1+4\gamma n^2\beta^2}\alpha_{302}\cos n\pi + \frac{16n^2\beta^2}{1+16\gamma n^2\beta^2}\alpha_{304} + \frac{36n^2\beta^2}{1+36\gamma n^2\beta^2}\alpha_{306}\cos n\pi\right)\right],\\
\alpha_{32} &= -\frac{1}{2(1-v^2)\beta^2}\left[\left(\frac{4n^2\beta^2}{1+4\gamma n^2\beta^2}\alpha_{302}\cos n\pi + \frac{16n^2\beta^2}{1+16\gamma n^2\beta^2}\alpha_{304} + \frac{36n^2\beta^2}{1+36\gamma n^2\beta^2}\alpha_{306}\cos n\pi\right)\right.\\
&\quad \left. - v\left(\frac{4m^2}{1+4\gamma m^2}\alpha_{320}\cos m\pi + \frac{16m^2}{1+16\gamma m^2}\alpha_{340} + \frac{36m^2}{1+36\gamma m^2}\alpha_{360}\cos m\pi\right)\right]\\
\alpha_{300} &= \frac{6}{\pi^2}\frac{C_{22}}{C_{211}K_1} + \frac{\pi^2}{12}(\alpha_{31}+\alpha_{32}) - 2\frac{K_2}{K_1}(\alpha_{31}+\beta^2\alpha_{32})
\end{aligned} \tag{A.2}$$

and for initially heated problem

$$\begin{aligned}
&A_{Mx}^{(0)} = A_{My}^{(0)} = -(1+v)\left(\frac{a}{t}\right)^2\alpha T_0 C, \quad C_{224} = C_{310} = C_{301} = C_{311} = 0\\
&C_1 = \frac{1}{6\pi^2}\frac{C_{01}}{C_{02}}, \quad C_2 = \frac{1-v^2}{18\pi^6}\frac{C_{22}}{C_{21}}\left(\frac{C_{01}}{C_{02}}\right)^4, \quad C_3 = \frac{1-v^2}{18\pi^6}\left(\frac{C_{01}}{C_{02}}\right)^3\\
&\alpha_{100} = \frac{6}{\pi^2}\frac{C_{02}}{C_{011}K_1} + \frac{\pi^2}{12}(\alpha_{11}+\alpha_{12}) - 2\frac{K_2}{K_1}(\alpha_{11}+\beta^2\alpha_{12})
\end{aligned} \tag{A.3}$$

and for initially compressed problem

$$\begin{aligned}
&A_{Mx}^{(0)} = A_{My}^{(0)} = 0\\
&C_1 = \frac{1}{6\pi^2}\frac{C_{01}}{B_{02}}, \quad C_2 = \frac{1-v^2}{18\pi^6}\frac{C_{22}}{C_{21}}\left(\frac{C_{01}}{B_{02}}\right)^4, \quad C_3 = \frac{1-v^2}{18\pi^6}\left(\frac{C_{01}}{B_{02}}\right)^3, \quad B_{02} = C_{02}\left(1 - \frac{B_{01}}{B_{011}}\frac{P_x}{P_{cr}}\right)\\
&C_{224} = \frac{\pi^2}{3}(\alpha_{31}+\alpha_{32})(m^2\alpha_{31} + \alpha_0 n^2\beta^2\alpha_{32})\left(\frac{C_{02}}{B_{011}}\right)\left(\frac{P_x}{P_{cr}}\right), \quad C_{310} = i^2m^2\left(\frac{C_{02}}{B_{011}}\right)\left(\frac{P_x}{P_{cr}}\right)\\
&C_{301} = \alpha_0 j^2 n^2\beta^2\left(\frac{C_{02}}{B_{011}}\right)\left(\frac{P_x}{P_{cr}}\right), \quad C_{311} = (i^2m^2 + \alpha_0 j^2 n^2\beta^2)\left(\frac{C_{02}}{B_{011}}\right)\left(\frac{P_x}{P_{cr}}\right)\\
&\alpha_{100} = \frac{6}{\pi^2}\frac{B_{02}}{C_{011}K_1} + \frac{\pi^2}{12}(\alpha_{11}+\alpha_{12}) - 2\frac{K_2}{K_1}(\alpha_{11}+\beta^2\alpha_{12}) + \frac{2}{K_1}(\alpha_{11}+\alpha_0\beta^2\alpha_{12})\frac{C_{02}}{B_{011}}\frac{P_x}{P_{cr}}
\end{aligned} \tag{A.4}$$

References

Akbarov, S.D., Kocatürk, T., 1997. On the bending problems of anisotropic (orthotropic) plates resting on elastic foundations that react in compression only. International Journal of Solids and Structures 34 (28), 3673–3689.

Bu, X.-M., Yan, Z.-D., 1991. Bending problems of rectangular Reissner plate with free edges laid on tensionless Winkler foundations. Applied Mathematics and Mechanics 12 (6), 605–616.

Celep, Z., 1988a. Circular plate on tensionless Winkler foundation. Journal of Engineering Mechanics ASCE 114 (10), 1723–1739.

Celep, Z., 1988b. Rectangular plates resting on tensionless elastic foundation. Journal of Engineering Mechanics ASCE 114 (12), 2083–2092.

Henwood, D.J., Whiteman, J.R., Yettram, A.L., 1982. Fourier series solution for a rectangular thick plate with free edges on an elastic foundation. International Journal for Numerical Methods in Engineering 18 (12), 1801–1820.

Hong, T., Teng, J.G., Luo, Y.F., 1999. Axisymmetric shells and plates on tensionless elastic foundations. International Journal of Solids and Structures 36 (34), 5277–5300.

Khathlan, A.A., 1994. Large-deformation analysis of plates on unilateral elastic foundation. Journal of Engineering Mechanics ASCE 120 (8), 1820–1827.

Li, Q.S., 2000. Buckling of flexural-shear plates. Journal of Engineering Mechanics ASCE 126 (12), 1466–1474.

Li, Q.S., 2001. Stability of tall buildings with shear wall structures. Engineering Structures 23 (9), 1177–1185.

Li, H., Dempsey, J.P., 1988. Unbonded contact of a square plate on an elastic half-space or a Winkler foundation. Journal of Applied Mechanics ASME 55, 430–436.

Mishra, R.C., Chakrabarti, S.K., 1996. Rectangular plates resting on tensionless elastic foundation: some new results. Journal of Engineering Mechanics ASCE 122 (4), 287–385.

Qu, Q., Liang, X., 1995. Nonlinear bending of rectangular plates with four free edges on elastic foundation. China Civil Engineering Journal 28 (1), 46–54 (in Chinese).

Shen, H.-S., 1998a. Thermal postbuckling analysis of imperfect Reissner–Mindlin plates on softening nonlinear elastic foundations. Journal of Engineering Mathematics 33 (3), 259–270.

Shen, H.-S., 1998b. Large deflection of Reissner–Mindlin plates on elastic foundations. Journal of Engineering Mechanics ASCE 124 (10), 1080–1089.

Shen, H.-S., 1999. Nonlinear bending of Reissner–Mindlin plates with free edges under transverse and in-plane loads and resting on elastic foundations. International Journal of Mechanical Sciences 41 (7), 845–864.

Shen, H.-S., 2001. Postbuckling of free edge Reissner–Mindlin plates elastically supported on a two-parameter foundation and subjected to biaxial compression and transverse loads. Engineering Structures 23 (3), 260–270.

Shen, H.-S., 2002. Postbuckling Behavior of Plates and Shells. Science and Technological Press, Shanghai, China (in Chinese).

Shi, X.P., Tan, S.A., Fwa, T.F., 1994. Rectangular thick plate with free edges on Pasternak foundation. Journal of Engineering Mechanics ASCE 120 (5), 971–988.

Silva, A.R.D., Silveira, R.A.M., Gonçalves, P.B., 2001. Numerical methods for analysis of plates on tensionless elastic foundations. International Journal of Solids and Structures 38 (10–13), 2083–2100.

Villaggio, P., 1983. A free boundary value problem in plate theory. Journal of Applied Mechanics ASME 50, 297–302.

Weitsman, Y., 1970. On foundations that react in compression only. Journal of Applied Mechanics ASME 37 (4), 1019–1030.

Xiao, J.R., 2001. Boundary element analysis of unilateral supported Reissner plates on elastic foundations. Computational Mechanics 27 (1), 1–10.

Yettram, A.L., Whiteman, J.R., Henwood, D.J., 1984. Effect of thickness on the behaviour of plates on foundations. Computers and Structures 19 (4), 501–509.